ORIGINAL PAPER

Binding free energy calculations of *N*-sulphonyl-glutamic acid inhibitors of MurD ligase

Andrej Perdih · Urban Bren · Tom Solmajer

Abstract The increasing incidence of bacterial resistance to most available antibiotics has underlined the urgent need for the discovery of novel efficacious antibacterial agents. The biosynthesis of bacterial peptidoglycan, where the MurD enzyme is involved in the intracellular phase of UDP-MurNAc-pentapeptide formation, represents a collection of highly selective targets for novel antibacterial drug design. Structural studies of *N*-sulfonyl-glutamic acid inhibitors of MurD have made possible the examination of binding modes of this class of compounds, providing valuable information for the lead optimization phase of the drug discovery cycle. Binding free energies were calculated for a series of MurD *N*-sulphonyl-Glu inhibitors using the linear interaction energy (LIE) method. Analysis of interaction energy during the 20-ns MD trajectories revealed non-polar van der Waals interactions as the main driving force for the binding of these inhibitors, and excellent agreement with the experimental free energies was obtained. Calculations of binding free energies for selected moieties of compounds in this structural class substantiated even deeper insight into the source of inhibitory activity. These results constitute new valuable information to further assist the lead optimization process.

Andrej Perdih and Urban Bren contributed equally to this work.

Electronic supplementary material The online version of this article (doi:10.1007/s00894-009-0455-8) contains supplementary material, which is available to authorized users.

A. Perdih · U. Bren · T. Solmajer (✉)
Laboratory for Molecular Modeling and NMR Spectroscopy,
National Institute of Chemistry,
Hajdrihova 19,
1001 Ljubljana, Slovenia
e-mail: tom.solmajer@ki.si

Introduction

In recent years the increasing incidence of bacterial resistance to most available antibiotics has made the discovery of novel efficacious antibacterial agents urgent [1]. In this process, novel previously unexploited targets are being considered [2]. As an essential bacterial component unique to prokaryotic cells, peptidoglycan is traditionally an optimal target with respect to selective toxicity [3]. The biosynthesis of peptidoglycan outlines a complex multi-stage process divided into early stages of intracellular assembly of UDP-MurNAc pentapeptide followed by a translocation step on the outercellular side and its final incorporation into the nascent biopolymer [4, 5]. Properly constructed peptidoglycan provides a prokaryotic cell with the rigidity, flexibility and strength that are indispensable for its growth and cell division, while withstanding high internal osmotic pressure [5].

Four ADP-forming bacterial ligases – MurC, MurD, MurE and MurF – are involved in the intracellular phase of peptidoglycan assembly, catalyzing the synthesis of a peptide moiety by consecutive addition of L-Ala, D-Glu, *meso*-DAP (or L-Lys) and D-Ala-D-Ala to the starting UDP-precursor (UDP-MurNAc) [6]. The Mur ligase family is outlined as a prime example of modular structure in protein architecture, with molecules made up of three domains or modules allowing for molecular recognition of the specific UDP-substrate (UDP-N-acetylmuramoyl group) [6]. The three-domain structure of the family comprises an

N-terminal domain primarily responsible for binding the UDPMurN-Ac substrate (e.g., UMA, UMAG, UMAN, etc.), a central domain bearing resemblance to the ATP-binding domains of a number of ATP- or GTP-ases and a C-terminal domain which is alleged to be involved in binding the incoming condensing amino acid [6]. All four ligases presumably act through an analogous sequential enzymatic mechanism, as corroborated by structural [7], biochemical [8, 9] and computational studies [10]. In the proposed mechanism, the bound UDP-precursor initially reacts with ATP to yield the acylphosphate intermediate, [10–12] which following the addition of the incoming amino acid affords the tetrahedral reaction intermediate [7, 10]. Finally, the dissociation of the phosphate group results in a new UDP-precursor elongated for the incoming amino acid.

The MurD (UDP-*N*-acetylmuramoyl-L-alanine:D-glutamate ligase) enzyme depicted in Fig. 1 is the second member of the bacterial Mur ligase series. It catalyzes an incorporation of D-Glutamate to the cytoplasmic intermediate UDP-*N*-acetyl-muramoyl-L-alanine (UMA), concomitant with the degradation of ATP to ADP and P_i [7]. Detailed X-ray structural investigations of the MurD ligase resulted in the identification of different protein conformations. The presence of "open" conformations of the enzyme suggests that binding of the ligands UMA and ATP is accompanied by the closure of the C-terminal domain to the catalytically active "closed form" [13]. The conformational closure of MurD has been computationally investigated by means of targeted molecular dynamics (TMD) simulations, providing a dynamic model of this process [14].

The attraction of this enzyme as a potential drug target resulted in the design of several MurD inhibitors [15]. One of the first published approaches was the design of transition state analogues based on the hypothetical structure of the enzyme's tetrahedral reaction intermediate. It was speculated that the placement of phosphonic acid between L-Ala and D-Glu would yield a structure closely

mimicking the proposed tetrahedral species [16]. Following the initial success of this approach, several low-molecular-weight analogues of the MurD tetrahedral intermediate possessing moderate inhibitory activity were published, mostly classified as phosphinate [17] and sulfonamide derivatives of D-Glutamic acid [18–20]. Although MurD ligase was previously established to be highly stereospecific for the D-Glu substrate [21], we were able to show that, surprisingly, it binds an inhibitor containing the L-Glu moiety [22, 23].

The geometry of the sulfonamide moiety is similar to the tetrahedral reaction intermediate formed during the cleavage or formation of the peptide bond and therefore represents a good starting point for the tetrahedral analogue design [24]. Recently, solved crystal structures of MurD complexes with *N*-sulfonyl derivatives of L- and D -Glutamic acid 1 (K_i=840 μM) and 2 (K_i=240 μM) provided the first possibility of observing the binding modes of this class of compounds [23]. In Fig. 1 the experimentally determined conformation of inhibitor 2, located between the UMA and D-Glu binding site of MurD, is shown. Furthermore, X-ray complexes of the two additional sulfonamide inhibitors 3 (IC_{50}=170 μM) and 4 (IC_{50}= 98 μM) depicted in Fig. 2 were solved, revealing virtually the same binding characteristics [20].

In addition, several inhibitors based on naphthalene *N*-sulfonyl derivatives of D-Glutamic acid were synthesized investigating the significance of various *O*-substitutions – compounds 5 (IC_{50}=810 μM), 6 (IC_{50}=590 μM), 7 (IC_{50}= 305 μM), and 8 (IC_{50}=239 μM) [19, 20]. Moreover, compound 9 (IC_{50}>2000 μM), in which the γ-carboxylic group is omitted, and several regioisomers (e.g., compound 10 with IC_{50}>1000 μM) were synthesized to further explore the behavior of this class of compounds. Some of the discovered inhibitors are considered as promising leads for further optimization. Therefore, several in silico compounds of the sulfonamide class with replacements of the

Fig. 1 Crystal structure of MurD enzyme complexed with *N*-sulphonyl-D-Glu inhibitor 2 (PDB code: 2JFF) [23] used in our LIE free energy simulation studies. *N*-terminal domain is denoted in yellow, central domain in blue and C-terminal domain in red. Bound inhibitor 2 is located between UMA and D-Glu binding site
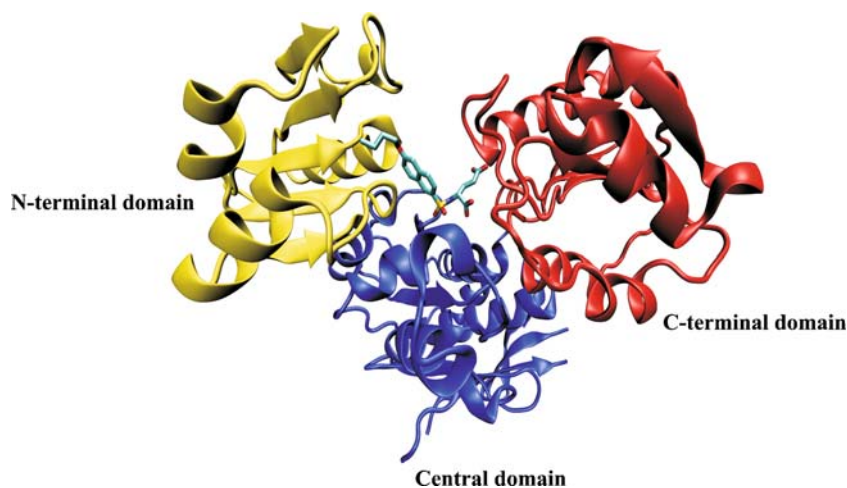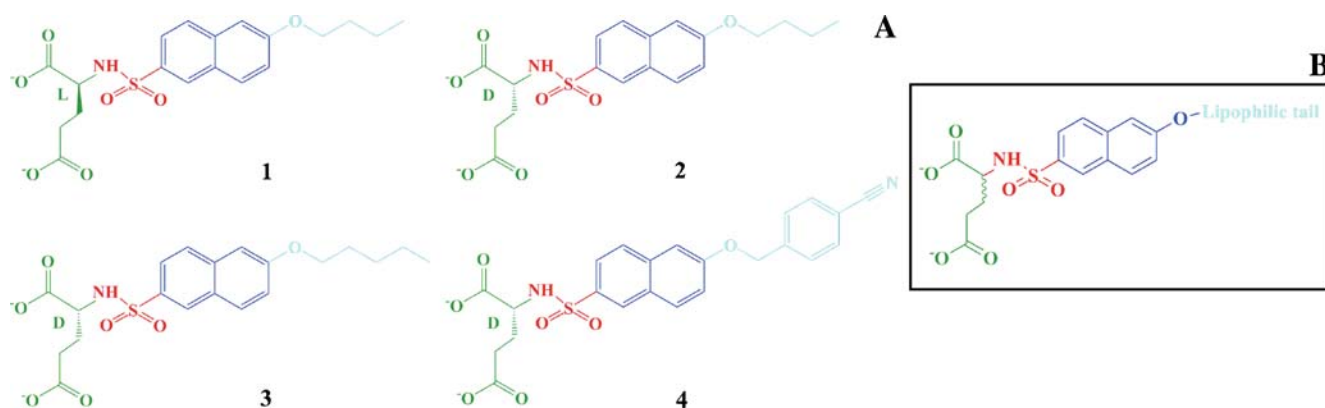
Fig. 2 (**a**) Chemical structures of *N*-sulphonyl-D-(or L-)Glutamic acid inhibitors of MurD **1–4** with experimentally determined binding modes used in our LIE studies [19–23]. (**b**) Dissection scheme of the generalized *N*-substituted glutamic acid inhibitor of MurD applied to calculate binding free energies of selected moieties

naphthalene scaffold or *O*-alkylated moiety were tested in molecular docking experiments taking advantage of the available crystal structures [22]. Molecules **11** and **12** represent examples of better ranked compounds. Detailed structural formulae for all studied molecular species are depicted in Table 2.

Computational chemistry combined with numerous structure-based drug design techniques comprises an essential part of the modern drug design process [25]. In particular, virtual screening (VS) experiments [26] utilizing available molecular docking [27] or pharmacophore modeling tools [28] to search for potential inhibitors in libraries of virtual or commercially available molecules are an integral part of the hit identification and lead optimization process. While by using most of the currently available molecular docking tools one is able to predict binding modes of investigated compounds with reasonable accuracy, calculations of binding free energies (directly corresponding to binding activities) still need to reach this level of confidence due to well known limitations of the available scoring functions [26]. In order to obtain accurate values of binding affinities, especially important in the lead optimization phase of the drug discovery process, rigorous methods have to be utilized [29]. Free energy perturbation (FEP) and thermodynamic integration (TI) are based on the construction of thermodynamic cycles and enable reliable predictions of binding free energies. On the other hand, they are computationally extremely time-consuming [30]. To find a compromise between accuracy and computational speed, Åqvist and co-workers developed the linear interaction energy (LIE) method [31, 32]. It was originally based on a modified linear response approximation for electrostatic interactions and on an empirical term treating non-polar interactions, which facilitates rapid free energy predictions. The LIE method later found wide application in numerous drug discovery projects [33–35]. More recently, in a generalized form of the LIE approach [36–40], both van der Waals parameter α and

electrostatic parameter β, previously fixed at a value of 1/2, are obtained by a fit of the calculated values of electrostatic and van der Waals interaction energies to the experimentally determined values of binding free energy for a set of known ligands [41, 42]. Many studies were able to derive models with typical errors of ∼ 1 kcal mol^{-1} between calculated and experimental absolute affinities. This level of accuracy is also what would be expected from the more rigorous, but computationally costlier, FEP or TI methods [43]. The ability to exactly decompose the free energy into contributions arising from different groups of atoms or types of interactions within the LIE formalism enables binding free energies of structural fragments comprising the investigated inhibitors to be determined as well [44].

In the present computational study we report the results of molecular dynamics simulations initiated to calculate binding free energies of a series of MurD *N*-sulphonyl-D-Glu inhibitors using the linear interaction energy (LIE) method. Twelve inhibitors of this chemical class were selected: four with experimentally determined binding mode and measured binding activity, six with experimentally determined binding activity and undetermined binding mode (among them four active and two inactive molecules), and two in silico molecules predicted to be favorable MurD inhibitors in molecular docking experiments. To gain even deeper insight into the source of inhibitory activity, binding free energies of selected compound moieties were calculated thereby providing novel information to support further drug design efforts.

Methods and computational strategies

Preparation of initial structures

Experimentally solved structures of the MurD enzyme co-crystallized with D-Glutamic acid inhibitors, which

represented the starting coordinates for our molecular dynamics simulations, were retrieved from the Protein Data Bank (PDB codes: 2JFF, 2JFH, 2UUO and 2UUP) [23, 45]. We would like to point out that these experimental crystal structures currently represent the only available structural data for this enzymatic system. The computational resources of the Beowulf-type CROW clusters at the National Institute of Chemistry in Ljubljana, Slovenia, were exploited in our free energy studies [46]. Preparation of the initial structures, as well as molecular dynamics simulations and free energy calculations, were performed with the Q program [47] developed by Åqvist and co-workers using the AMBER force field [48].

Initial complexes of molecules with unknown binding modes were constructed by manually modifying the structure of inhibitor 2 in 2JFF crystal structure yielding complexes 5–7 and 9–10, or inhibitor 4 in 2UUP crystal structure yielding the complex 8. In compounds 5–8 the O-substituted side chain was modified. γ-carboxylate side chain of compound 2 was deleted to obtain compound 9. For compound 10, D-Glu and the sulfonamide moiety were kept in their original 2JFF position and the 1,5 naphthalene moiety was positioned in the bulk. The 2JFF complex served as a starting point for the construction of in silico compounds 11 and 12 as well [22].

To begin with, the empirical force field parameters for all inhibitors and carbamylated Lys198 (KCX198) residue had to be developed. In order to calculate partial atomic charges, all ligands were extracted from their complexes and hydrogen atoms were added using an algorithm incorporated in the Spartan software [49]. The obtained structures were subjected to full geometry optimization and subsequent vibrational analysis in the harmonic approximation at the Hartree-Fock (HF) level of theory using 6-31G(d) basis set encoded in the Gaussian 03 program [50]. The absence of imaginary vibrational frequencies indicated correctly performed minimizations [51]. The RESP charge-fitting procedure was initiated to reproduce the HF/6-31G (d) calculated electrostatic potential (ESP) surrounding the inhibitors [52]. Partial charges of chemically equivalent atoms were restricted to the same value. Standard van der Waals parameters were applied due to large transferability between molecules. Missing stretching, bending, dihedral and improper dihedral parameters required for the complete description of the inhibitors were taken from the Generalized AMBER Force Field (GAFF) [48]. Force field parameters of the carbamylated Lys198 (KCX198) side chain were prepared using the same procedure. Partial atomic charges and atom types developed for all 12 inhibitors and KCX residue are listed in the Supplementary material.

All crystal waters were deleted from the complex and a system representing the ligand's bound state was prepared by constructing a sphere of TIP3P [53] water molecules with a radius of 25 Å centered on the bridging O22 atom.[1] Water molecules that sterically overlapped with the atoms in the crystal structure were deleted. The configuration of the ligand's free-state was prepared by constructing a sphere of TIP3P water molecules around the ligand, again with a radius of 25 Å and centered on the bridging O22 atom*. Protonation of the ionizable amino acid residues was assigned by the following rules: side chains of Asp, Glu and KCX residues located within 22 Å of the sphere center were treated as negatively charged. Similarly, side chains of Lys and Arg residues were treated as positively charged. In the area between 22 Å and 25 Å away from the sphere center, the ionizable residues were generally treated as neutral entities. In the case of an identified salt bridge, both of the interacting partners were charged. Histidine residues located within 22 Å of the sphere center were assigned their protonation pattern in the last stage to approach the electroneutrality of the system as closely as possible. All ionizable side chains outside of the simulation sphere were modeled as uncharged entities. In our MD simulations, the following residues were considered charged: Arg (32, 37, 52, 100, 186, 200, 302, 371, 425), Lys (45, 115, 319, 348, 420), Asp (2, 35, 44, 59, 94, 182, 185, 317, 346, 372, 417), Glu (51, 90, 96, 157, 164, 181, 388, 423, 428), His (53, 78, 183, 310). The sum of their total charges together with the KCX residue (total charge of -1) and the inhibitor's total charge of -2 (-1 in the case of compound 9) required the addition of 5 (or 4) sodium ions in the bound state to make the system electroneutral. In the free state, 2 (or 1) sodium ions were included for this purpose. Topology and coordinate files necessary for the initiation of molecular dynamics simulations were generated using the Qprep5 program.

Molecular dynamics simulations

The configurational ensembles that served for the evaluation of binding free energies were generated by molecular dynamics (MD) simulations. The systems were subjected to surface constraint all atoms solvent (SCAAS) spherical boundary conditions, which mimic the infinite aqueous solution [54]. Protein atoms protruding beyond the 25 Å sphere boundary were restrained to their coordinates from the crystal structure using harmonic constraints. Non-bonding interactions of these atoms were turned off. Other non-bonding interactions were explicitly evaluated for distances under 10 Å. The local reaction field (LRF) method was used to treat long-range electrostatics for

---

[1] or corresponding hydrogen in compound 5

distances beyond the 10 Å cut-off [55]. A restraining harmonic potential with a force constant of 100 kcal/(mol Å^2) was applied to the position of the O22 atom for all investigated ligands in their free state. The position of sodium ions was restrained by a 75 kcal/(mol Å^2) flat-bottom harmonic potential that was set to zero for distances less than 21.5 Å from the center of the simulation sphere. These potentials were applied to prevent diffusion of inhibitors and sodium ions toward the edge of the simulation sphere.

All systems were first optimized by 30000- and 20000-step MD simulations at 5 K with a step size of 0.005 and 0.01 fs, respectively. In systems representing the bound state, the coordinates of protein and ligand heavy atoms were constrained, allowing only for water relaxation, as opposed to the free state, where the inhibitor atoms were allowed to move freely. In further stages the whole system was relaxed at 5 K by a series of four 20000- and one 50000-step simulations with increasing step size (step size prolongation program: 0.01 fs, 0.04 fs, 0.1 fs, 0.3 fs and 1 fs). Subsequent heating of the simulated system from 5 K to 298 K was performed by a series of six MD simulations with a 1 fs step size (temperature heating program: 50 K, 100 K, 150 K, 200 K, 250 K, 298 K), comprising 300 to 330 ps of total simulation time. A 200 ps MD simulation at 298 K using a 2 fs step size with the SHAKE algorithm applied to bonds involving hydrogen atoms yielded the starting structure for the production phase.

Production trajectories generated (N, V, T) ensembles at 298 K. The NVT ensemble (canonical ensemble) keeps the number of moles, the volume, and the temperature fixed [56]. The integration step was 2 fs and the SHAKE algorithm was applied to bonds involving hydrogen atoms. The energy of the system was sampled at every 10th step. To evaluate the binding free energies of selected moieties, molecules **1–12** were decomposed into 4 regions, as shown for the generalized inhibitor structure in Fig. **2** b. The first moiety consisted of glutamate residue without the amino group; the second included 5 atoms of the sulfonamide group. A naphthalene ring and the bridging oxygen encompassed the third moiety. The fourth moiety covered various lipophilic substituents appearing in the studied molecules. Production runs of 5 ns were initiated from 4 independent starting configurations (obtained by the heating protocols of 300, 310, 320, 330 ps length which resulted in these different configurations, respectively). This resulted in 20 ns of total production run for each of the investigated systems. Standard deviations were calculated from four independent 5 ns MD production run simulations which were initiated from four different starting configurations. Visualization and analysis of production trajectories were performed using the VMD 1.8.6 program [57].

LIE – Linear interaction energy method

The linear interaction energy (LIE) approach of Åqvist and co-workers represents a rapid method of evaluating binding free energies. It is based on a modified linear response approximation for electrostatic interactions and on an empirical term treating the non-polar interactions [32]. Its significant advantage is that only MD simulations of two physical states – the bound and free state of an investigated ligand – have to be performed, which reduces computational expense coupled with FEP or TI methods [29]. The thermodynamic cycle employed in our LIE calculations is depicted in Fig. **3**.

Since free energy is a state function, the sum of free energy changes represented in a thermodynamic cycle has to be zero:

$$\Delta G_{binding} + \Delta G_{decoupling}^P - \Delta G_{decoupling}^W - \Delta G_{binding}^{decoupled} = 0 \tag{1}$$

A decoupled ligand has all non-bonding interactions switched off and its binding free energy $\Delta G_{binding}^{decoupled}$ equals zero. Therefore, Eq. (1) can be reconfigured as:

$$\Delta G_{binding} = \Delta G_{decoupling}^W - \Delta G_{decoupling}^P. \tag{2}$$

The decoupling terms are actually free energy differences accompanying the transfer of a ligand from either aqueous solution (free state W) or solvated receptor binding site (bound state P) to a vacuum [32]. The corresponding solvation free energies are in the framework of the LIE methodology expressed as:

$$\Delta G_{solvation}^Q = -\Delta G_{decoupling}^Q = \alpha \left\langle V_{L-Q}^{vdW} \right\rangle + \beta \left\langle V_{L-Q}^{ES} \right\rangle \tag{3}$$

where $\left\langle V_{L-Q}^{vdW} \right\rangle$ and $\left\langle V_{L-Q}^{ES} \right\rangle$ represent van der Waals and electrostatic interaction energy between ligand L and its surrounding Q – either aqueous solution W or solvated binding site P – averaged over the ensemble of configurations generated by MD simulation. Using relations (2) and (3), binding free energy can be obtained as:

$$\Delta G_{binding} = \alpha \left(\left\langle V_{L-P}^{vdW} \right\rangle - \left\langle V_{L-W}^{vdW} \right\rangle \right) + \beta \left(\left\langle V_{L-P}^{ES} \right\rangle - \left\langle V_{L-W}^{ES} \right\rangle \right) \tag{4}$$

The optimized values of empirical coefficients of the LIE method α and β were obtained by generating a RMSD function between the interaction energies expressed as a function of both empirical coefficients α and β and the experimental binding free energies over the series of *N*-sulphonyl-D-Glu inhibitors **2–10** with experimentally determined binding affinities [38, 41, 42]. The minimum of this function at 0.19 kcal mol^{-1} corresponds to the optimal
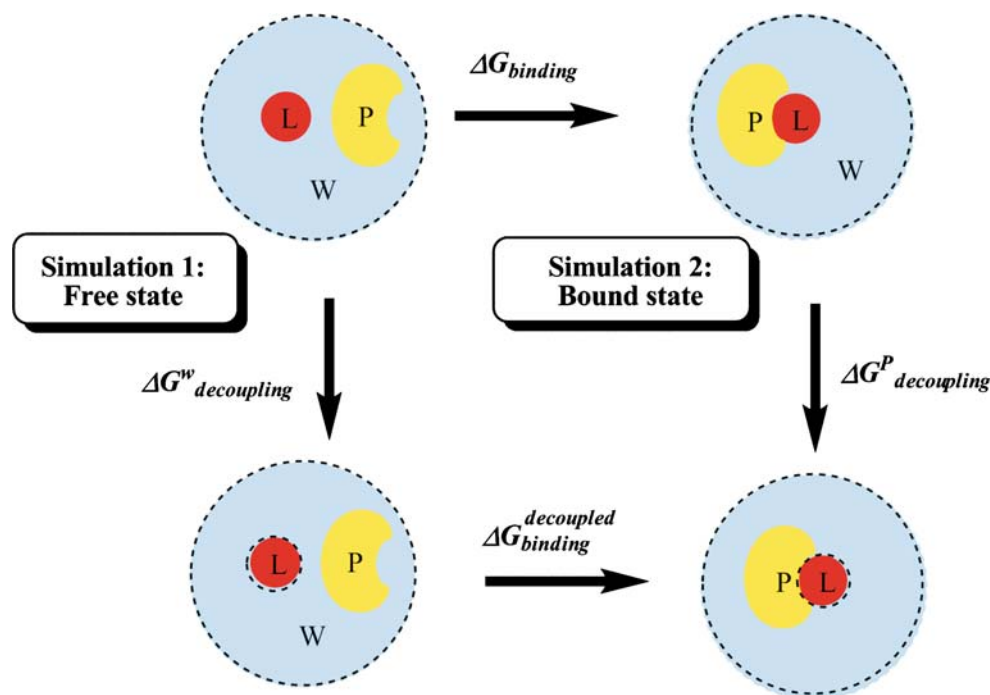
LIE parameters $\alpha=0.176$ and $\beta=0.060$. In the coefficients fitting procedure a smaller set of compounds was also considered, using selected N-sulphonyl-D-Glu inhibitors **2–4**. The difference between the α and β values obtained on the larger and smaller set was negligible (smaller set yielded LIE parameters $\alpha=0.175$ and $\beta=0.068$), indicating the stability of the LIE coefficients for the studied sulfonamide chemical class. In addition, it was gratifying to observe that the value of α compares favorably with the value of 0.18 – previously derived in a variety of enzymatic systems [39–42]. In two very recent studies on protein kinase CDK2 [41] and protein kinase CK2 [42] inhibition, evidence is presented that electrostatic parameter β of 0.05 and 0.08 yielded the best statistics for models developed on a large number of inhibitors.

In the case of classical force fields, interaction energy V can be exactly decomposed into contributions of all atom groups present. Since binding free energy is in Eq. (4) expressed as a linear combination of interaction energies, the binding free energies of selected moieties can be explicitly evaluated within the LIE formalism.

Results and discussion

### Analysis of interaction energy obtained from MD simulations

Interaction energies between ligands **1–12** and their surroundings were calculated using the Qfep5 program for the free and the bound states. The time dependence of the interaction energy for the sulfonamide MurD inhibitor **3** in the bound and free state (available in Fig.15 of the Supplementary material) consists of four 5 ns MD simulations initiated from four independent starting configurations to representatively cover the available conformational space. The analysis of interaction energy demonstrated that the binding of compound **3** is energetically favored, with the interaction energy fluctuating considerably in both states. This is not surprising, as the investigated sulfonamide inhibitors (with the exception of compound **5**) possess two charged carboxylic groups with a total charge of -2. Nearly identical behavior of the interaction energy during the course of MD simulation was observed for the remaining inhibitors in the series.

To gain deeper insight into the physicochemical origin of inhibitor binding, the electrostatic and van der Waals components of the interaction energy were plotted separately as a function of time for both simulated states of compound **3** (Fig. 4). The van der Waals interaction energy fluctuates between -10 kcal mol^{-1} and -20 kcal mol^{-1} in the free state and between -35 kcal mol^{-1} and -50 kcal mol^{-1} in the bound state, respectively. Therefore, in terms of the van der Waals component a clear preference for the bound state can be observed.

The electrostatic interaction energy between compound **3** and its surroundings fluctuates between -400 kcal mol^{-1} and -500 kcal mol^{-1}. Therefore, the electrostatic component represents the main origin of significant fluctuations in the overall interaction energy. On the other hand, the

Fig. 4 Interaction energy decomposition for compound **3**: van der Waals (**a**) and electrostatic (**b**) energy component between inhibitor **3** and its surrounding (water and sodium ions in the **free state** (blue) and water, sodium ions and protein in the **bound state** (red)) during the 20 ns MD simulation
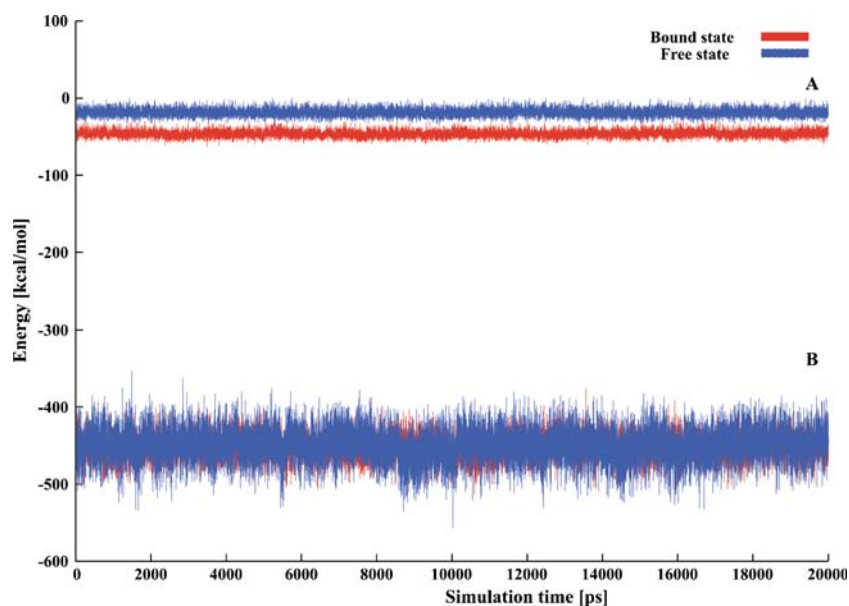
average electrostatic interaction energy and the extent of its fluctuations are virtually identical in the bound and in the free state of compound **3**. Similar behavior was observed for the remaining 11 MurD inhibitors, leading to the conclusion that the van der Waals component represents the main driving force for binding and a prerequisite for inhibitory activity of these compounds.

This finding is in accordance with the high plasticity observed in the Mur ligase family of enzymes where huge conformational changes in the enzyme structure were detected [13, 14]. Additional corroboration is provided by the predomination of negatively charged residues in the binding site of MurD, although this enzyme binds negatively charged substrates. The vast surface of the MurD substrate binding site [7] and the experimental observation that the sulfonamide inhibitor (except for the D-Glu moiety) interacts with the enzyme through indirect interactions [23] are in accord with obtained interaction energy results which indicate that the entropic contribution to binding plays a predominant role in the case of these inhibitors.

In the LIE formalism, binding free energy is calculated as the weighted difference between the average electrostatic and van der Waals interaction energies of the ligand in the bound and in the free state – Eq. (4). For each of the 12 inhibitors studied, the electrostatic term contributing to the binding free energy in Eq. (4) is consistently much smaller than the van der Waals contribution.

Binding free-energy calculations

The average van der Waals and electrostatic interaction energies of the ligands in the bound and in the free state obtained from MD simulations are collected in Table 1. Experimental binding free energies of compounds were calculated by the standard thermodynamic relation

$$\Delta G_{binding} = RT \ln(K_i) \tag{5}$$

where R, T and K_i represent universal gas constant, thermodynamic temperature and experimental dissociation constant, respectively. Binding free energies of investigated inhibitors **1–12** calculated by using optimized empirical coefficients 0.176 (α) and 0.060 (β) of the LIE equation (4) are assembled in Table 2 along with their experimental counterparts for comparison.

The experimental binding free energy of compound **1** (L-Glu isomer) is −4.4 kcal mol^{-1}, whereas our LIE simulation predicts a value of −5.1±0.9 kcal mol^{-1}, which is still close to the experimental value considering the high value of standard deviation. Compound **2** represents the D-stereoisomer of compound **1** with a more favorable experimental binding free energy of −4.9 kcal mol^{-1} due to the intrinsic preference of the MurD enzyme for the substrate D-Glu as a precursor for the growing polypeptide chain of the UDP-molecule [22]. The calculated binding free energy was −4.9±0.3 kcal mol^{-1}. The plausible explanation of the larger standard deviation observed for compound **1** is provided by the comparison of conformations of stereoisomers **1** and **2** containing L-Glu and D-Glu moiety (plots of RMS deviation from the conformation in the experimental crystal structure during MD simulation are given in the Supplementary material), which shows that the L-Glu inhibitor fluctuates between two conformations while D-Glu inhibitor remains firmly anchored close to its position in the crystal structure. The additional methyl group in the lipophilic tail of compound **3** contributes

Table 1 Average van der Waals and electrostatic interaction energy between *N*-sulfonyl-glutamic acid inhibitors **1–12** and their surrounding (solvated receptor P or aqueous solution W) obtained from MD simulations

Compound	$\langle V_{L-P}^{vdW} \rangle$ [kcal mol^{-1}]	$\langle V_{L-W}^{vdW} \rangle$ [kcal mol^{-1}]	$\langle V_{L-P}^{vdW} \rangle - \langle V_{L-W}^{vdW} \rangle$ [kcal mol^{-1}]	$\langle V_{L-P}^{el} \rangle$ [kcal mol^{-1}]	$\langle V_{L-W}^{el} \rangle$ [kcal mol^{-1}]	$\langle V_{L-P}^{el} \rangle - \langle V_{L-W}^{el} \rangle$ [kcal mol^{-1}]
1	−41.7±3.3	−17.2±0.1	−24.5±3.4	−460.2±2.4	−446.4±2.4	−13.7±4.8
2	−43.5±0.5	−17.2±0.1	−26.2±0.6	−452.8±1.2	−447.7±1.6	−5.1±2.8
3	−46.3±0.3	−18.6±0.1	−27.7±0.4	−452.0±0.4	−449.6±1.6	−2.4±2.0
4	−51.9±0.8	−20.7±0.1	−31.2±0.9	−450.5±1.4	−447.0±2.3	−3.5±3.7
5	−30.5±0.3	−8.8±0.1	−21.7±0.4	−454.2±3.9	−445.8±1.3	−8.4±5.2
6	−33.4±0.5	−12.0±0.3	−21.4±0.8	−458.8±6.7	−451.8±1.5	−7.0±8.2
7	−41.3± 1.1	−15.5±0.1	−25.8±1.2	−456.5±6.8	−448.7±4.7	−7.8±11.5
8	−45.9±1.7	−19.3±0.1	−26.6±1.8	−457.2±1.8	−449.2±1.6	−8.0±3.4
9	−39.2±1.2	−21.7±0.1	−17.5±1.3	−193.3±4.2	−178.2±0.4	−15.0±4.6
10	−39.6±1.3	−16.5±0.2	−23.1±1.5	−451.4±3.0	−445.6±1.6	−5.9±4.6
11	−45.7±0.9	−18.0±0.2	−27.7±1.1	−449.1±3.2	−443.0±2.2	−6.1±5.4
12	−48.9±2.6	−20.3±0.2	−28.6±2.8	−474.7±5.0	−461.4±1.5	−13.3±6.5

Standard deviations were calculated from four 5 ns MD simulations which were initiated from four independent starting configurations

favorably by decreasing the experimental binding free energy to −5.2 kcal mol^{-1}, which concurs with the LIE binding free energy of −5.0±0.2 kcal mol^{-1}. The incorporation of the lipophylic 4-cyano phenyl moiety resulted in compound **4**, with an experimental binding free energy of −5.5 kcal mol^{-1}.

Inhibitors **5–8** comprise a set of active compounds where binding free energies occupy values between -4.3 and −5.0 kcal mol^{-1}. The results of the LIE simulations are in excellent agreement with the experiment as calculated binding free energies rest between −4.2±0.7 and −5.2±0.5 kcal mol^{-1} (Table 2). For compounds **9** and **10**, with substantially lower inhibitory activities, experimental binding free energy could only be determined from a lower boundary of the IC$_{50}$ value [18]. Compound **9**, lacking the γ-carboxylic side chain, exhibits the weakest binding in the series, with an experimental binding free energy higher than −3.7 kcal mol^{-1}. The LIE simulations predicted −4.0±0.5 kcal mol^{-1}. The experimental binding free energy of compound **10** (regioisomer of compound **2**) is estimated as higher than −4.1 kcal mol^{-1}. The LIE result of −4.4±0.5 kcal mol^{-1} agrees nicely with the experiment.

In silico compounds **11** and **12** were proposed by the use of molecular docking as further optimization possibilities of this class of inhibitors [20, 22]. These compounds explore substitution of the naphthalene ring or of the lipophilic tail to further enhance ligand-protein interactions. As the generation of ligand-protein complex structures in molecular docking experiments involves the use of a less reliable scoring function, LIE simulations could offer additional confirmation of the predicted favorable binding properties. The introduction of 4-methylquinazoline as a surrogate of naphthalene in compound **11** was estimated to result in a binding free energy of −5.2±0.9 kcal mol^{-1}. The replacement of the 4-cyano phenyl group of inhibitor **4** with
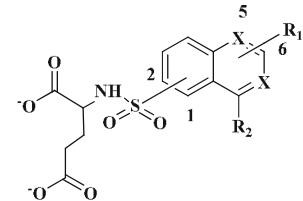
2*H*-1,3-thiazine-2,6(3*H*)-dione yields compound **12**, with a predicted binding free energy of −5.8±0.9 kcal mol^{-1}. In summary, the results of the LIE simulations indicate that the proposed in silico replacements would not considerably improve the binding free energy, yielding molecules with inhibitory activity similar to already synthesized inhibitors.
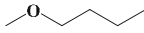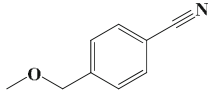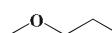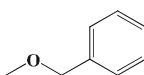
The results of our free energy simulations, making use of the MurD optimized values of empirical LIE coefficients, are well in accordance with the available experimental data. The correlation graph between the calculated (with error bars) and experimental binding free energies for compounds **1–10** with the available experimental inhibitory activities is shown in Fig. 5, yielding a correlation coefficient r^2 of 0.86 and a RMSE (root mean square error) of 0.53. The Leave-more-out cross-validation 30% procedure [58] yielded a 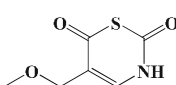cross-validated r^2 (q^2) of 0.84 and a cross-validated RMSE of 0.51. The quality of this agreement provides additional confidence in predicted binding free energies for in silico compounds **11** and **12**.

Binding free energies of selected moieties

Within the framework of the LIE methodology, free energy can be exactly decomposed into contributions arising from different groups of atoms or types of interactions. Decomposition of the binding free energies yields contributions of specific moieties to overall inhibitory activity (Table 3), which are especially important for the currently undergoing optimization phase of MurD inhibitors in the series.

The binding free energy of the glutamic acid moiety without the nitrogen atom varies within a small interval between −2.2±0.2 and −2.7±0.5 kcal mol^{-1}, indicating a similar role of this residue throughout the inhibitor series. Compound **9** yields a considerably smaller partial binding

Table 2 Calculated binding free energies of *N*-sulfonyl-glutamic acid inhibitors **1–12** compared with the available experimental results

Compound	R₁	R₂	X	Substitution	IC₅₀[**] [μM]	ΔG_binding^exp. [kcal mol⁻¹]	ΔG_binding^calc. [*****] [kcal mol⁻¹]
1[*]	~O~~~	H	C,C	2,6	710	-4.4	-5.1 ± 0.9
2	~O~~~	H	C,C	2,6	280	-4.9	-4.9 ± 0.3
3	~O~~~~	H	C,C	2,6	170	-5.2	-5.0 ± 0.2
4	(4-cyanobenzyl ether)	H	C,C	2,6	105	-5.5	-5.7 ± 0.4
5	**–H**	H	C,C	2,6	810	-4.3	-4.3 ± 0.4
6	~O~	H	C,C	2,6	590	-4.5	-4.2 ± 0.7
7	~O~~	H	C,C	2,6	305	-4.9	-5.0 ± 0.9
8	(benzyl ether)	H	C,C	2,6	239	-5.0	-5.2 ± 0.5
9[***]	~O~~~	H	C,C	2,6	>2000	>-3.7	-4.0 ± 0.5
10	~O~~~	H	C,C	1,5	>1000	>-4.1	-4.4 ± 0.5
11[****]	~O~~~	CH₃	N,N	2,6	/	/	-5.2 ± 0.9
12[****]	(thiouracil ether)	H	C,C	2,6	/	/	-5.8 ± 0.9

[*]   L-Glu (in other cases, except compound **9**, D-Glu)
[**]   For compounds 1-10 experimental binding free energy was calculated from the measured
         IC₅₀ values. Steady-state kinetics revealed IC₅₀ values of structurally related compounds 1 and 2
         to be in a good agreement with the measured K_i [23]
[***]   γ-carboxylate is omitted
[****] *In silico* compounds not yet synthesized
[*****] Standard deviations were calculated from four 5 ns MD simulations which were initiated from four
         independent starting configurations.

free energy of -1.5 ± 0.2 kcal mol⁻¹, confirming the importance of the γ-carboxylic group for inhibitory activity.

The binding free energy of the sulfonamide moiety ranges between -0.7 ± 0.2 and -0.9 ± 0.2 kcal mol⁻¹, making a significant contribution to the overall binding affinity. The naphthalene moiety with the bridging oxygen O22 (except in compound **5**, which lacks O22) has binding free energies between -0.9 ± 0.1 and -1.2 ± 0.2 kcal mol⁻¹. Replacement of the naphthalene moiety by 4-methylquinazoline in compound **11** leads to a similar value of partial binding affinity.

The most diverse binding contributions originate from the lipophilic tail, which in compounds **1**, **2** and **9–11** consists of a butyl group. Our results reproduce the order of inhibitory activities for compounds **2–4** with experimentally determined crystal structures, where all structural differences between ligands originate from this moiety. Lipophilic tail contribution also favors compound **2** (-0.9 ± 0.1 kcal mol⁻¹) over its L-stereoisomer **1** (-0.6 ± 0.3 kcal mol⁻¹), in accordance with the intrinsic nature of the MurD enzyme to bind D-Glu ligands. The additional
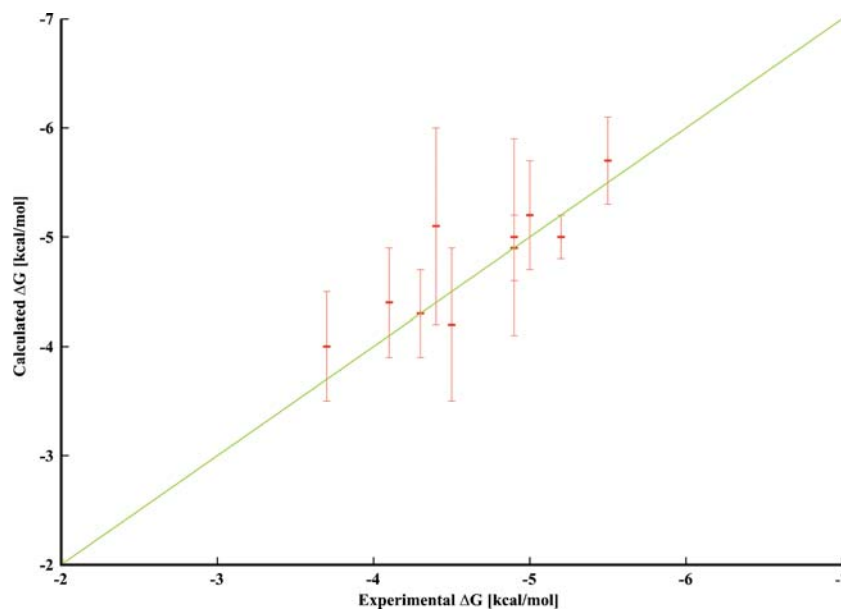
methyl group in the lipophilic tail of compound **3** contributes favorably by increasing its partial binding free energy. Compounds **6** and **7** with shorter aliphatic chain bear smaller binding contributions of -0.1 ± 0.1 and -0.7 ± 0.2 kcal mol^{-1}. The incorporation of the 4-cyano phenyl group in the lipophilic moiety of compound **4** results in the most potent binding contribution of -1.4 ± 0.2 kcal mol^{-1}.

Analysis of MD trajectories

The MD trajectories of all ligands in the bound state provide a considerable amount of structural data for further

analysis. Table 4 shows the average distances of important interactions between inhibitors and MurD amino acid residues. The time dependence of all selected distances and animation of compound **4** in the bound state during MD simulation are available in the Supplementary material. Interactions of Thr321 and Lys348 with Glu α-carboxylate, of Ser415 and Phe422 with Glu γ-carboxylate, as well as of His183 with the sulfonamide moiety, were monitored for all compounds (with the exception of compound **9**, which does not possess the γ-carboxylate). For compounds **4** and **12**, additional distances between Thr36 and the lipophilic tail were measured.

The average distances demonstrate little deviation in the length of hydrogen bonds between MurD residues and γ-

Table 3 Decomposition of binding free energies for inhibitors **1–12**. Standard deviations were calculated from four 5 ns MD simulations which were initiated from four independent starting configurations

Compound	$\Delta G_{binding}^{D-Glu}$ [kcal mol^{-1}]	$\Delta G_{binding}^{Sulphonamide}$ [kcal mol^{-1}]	$\Delta G_{binding}^{Naphthalene}$ [kcal mol^{-1}]	$\Delta G_{binding}^{Tail}$ [kcal mol^{-1}]
1*	−2.7±0.5	−0.9±0.2	−1.0±0.2	−0.6±0.3
2	−2.3±0.2	−0.8±0.1	−0.9±0.1	−0.9±0.1
3	−2.2±0.2	−0.8±0.1	−1.0±0.1	−1.1±0.2
4	−2.6±0.3	−0.8±0.2	−1.0±0.2	−1.4±0.2
5	−2.7±0.3	−0.8±0.1	−0.9±0.1	/
6	−2.4±0.6	−0.8±0.2	−1.0±0.1	−0.1±0.1
7	−2.5±0.6	−0.8±0.2	−1.0±0.1	−0.7±0.2
8	−2.7±0.2	−0.8±0.1	−1.0±0.1	−0.6±0.4
9**	−1.5±0.2	−0.9±0.1	−1.0±0.1	−0.6±0.3
10	−2.4±0.4	−0.7±0.2	−0.9±0.1	−0.4±0.2
11***	−2.5±0.3	−0.8±0.2	−1.1±0.1	−0.9±0.2
12	−2.6±0.3	−0.9±0.1	−1.2±0.2	−1.2±0.6

* L-Glu

** γ-carboxylate is omitted

*** The naphthalene moiety is replaced by 4-methylquinazoline moiety

Table 4 The average MD distances between compounds **1–12** and selected MurD residues: (a) side chain oxygen of Thr321 and α-carboxylic oxygen of **1–12** (b) side chain nitrogen of Lys348 and α-carboxylic oxygen of **1–12** (c) backbone nitrogen of Ser415 and γ-carboxylic oxygen of **1–8** and **10–12** (d) side chain oxygen of Ser415 and γ-carboxylic oxygen of **1–8** and **10–12** (e) backbone nitrogen of Phe422 and γ-carboxylic oxygen of **1–8** and **10–12** (f) ND1 nitrogen of His183 and oxygen of **1–12** sulfonamide moiety (g) NE2 nitrogen of His183 and oxygen of **1–12** sulfonamide moiety (h) backbone nitrogen of Thr36 and cyano nitrogen of **4** or carbonyl oxygen of **12** (i) side chain oxygen of Thr36 and ciano nitrogen of **4** or amide nitrogen of **12**

Comp.	Thr321 [Å]	Lys348 [Å]	Ser415 (N) [Å]	Ser415 (O) [Å]	Phe422 [Å]	His183 (1) [Å]	His183 (2) [Å]	Thr36 (N) [Å]	Thr36 (O) [Å]
1	4.30	3.77	2.87	2.70	3.14	3.65	4.74	/	/
2	4.24	2.74	2.83	2.64	2.93	3.43	4.97	/	/
3	4.34	2.85	2.84	2.64	2.90	3.31	5.22	/	/
4	3.52	2.92	3.04	2.97	3.02	4.32	6.14	3.36	3.04
5	4.02	2.74	3.25	2.80	3.32	3.30	5.08	/	/
6	3.93	2.83	2.84	2.69	2.93	3.67	5.60	/	/
7	4.13	2.78	2.83	2.91	2.93	3.46	5.19	/	/
8	3.88	2.80	2.89	2.70	3.12	3.59	5.52	/	/
9	4.31	4.54	/	/	/	3.70	5.43	/	/
10	3.77	3.77	2.92	2.71	2.99	3.72	5.43	/	/
11	4.40	3.39	2.85	2.64	2.94	3.44	4.82	/	/
12	3.69	3.16	2.84	2.65	3.01	3.73	5.39	6.23	5.30

carboxylate in compounds **1–8** and **10–12**. Distances to the backbone nitrogen (2.83–3.25 Å) and side chain oxygen (2.64–2.97 Å) of Ser415, as well as to the side chain nitrogen of Phe422 (2.90–3.32 Å), all deviate within 0.4 Å, signifying the importance of γ-carboxylate for successful molecular recognition. Much less uniformity can be observed in the interactions between Lys348 and α-carboxylate. In compound **1** the apparently less favorable stereochemical orientation of α-carboxylate results in a longer H-bond with Lys348 (3.77 Å), which corroborates well with weaker binding affinity. A similar deviation can be observed for compound **9**, where the absence of γ-carboxylate produces a negative influence on the interaction

with Lys348 (4.54 Å). Crystal structures of MurD inhibitors revealed that Thr321 interacts with Glu α-carboxylate *via* the connecting water molecule [23]. Larger average distances of this interaction (3.52–4.40 Å) agree nicely with this experimental observation.

The distances between His183 and both oxygen atoms of the sulfonamide moiety were monitored. In the structural studies this interaction was only observed for L-stereoisomer **1** *via* the connecting water molecule W172 [23]. The time dependence of the distance between the sulfonamide oxygen of inhibitor **1** and His183 ND1 nitrogen is depicted in Fig. 6. The presence of two distinct conformations is clearly indicated – one representing direct and the other water-

Fig. 6 Time-dependence of distance between ND1 nitrogen of His183 and O32 oxygen of the sulfonamide moiety in compound **1**
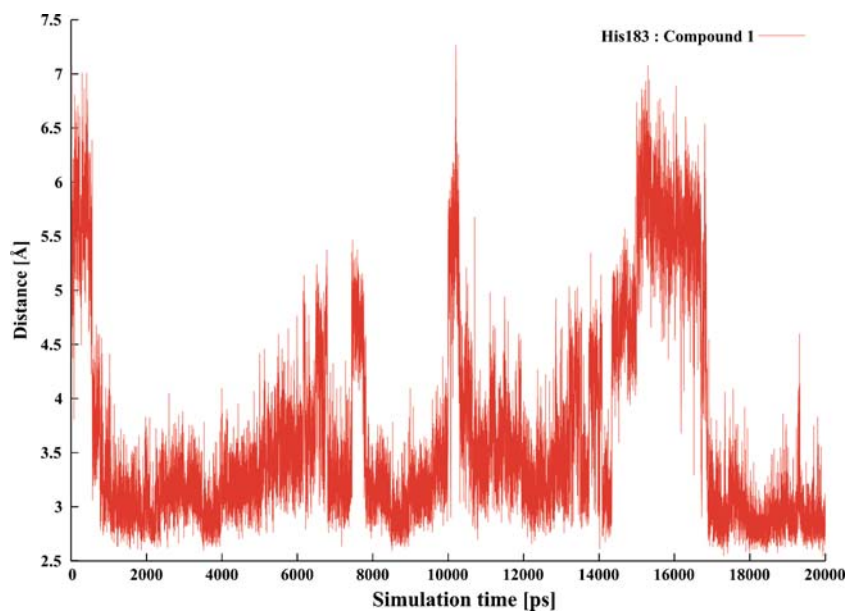
mediated interaction. Average lengths of this interaction range between 3.30 and 3.73 Å (with the exception of compound **4**), suggesting a possible role of His183 in optimal inhibitor recognition through either direct or indirect interaction.

The naphthalene moiety was significantly mobile during the MD simulations. This can be nicely observed in the dynamic animation of compound **4**, available in the Supplementary material. Eight of the 12 studied inhibitors contain a flexible lipophilic tail composed of one to five aliphatic carbon atoms, which are able to interact with the uracil part of the UMA binding site. Aliphatic tails were found to occupy numerous conformations throughout the MD simulations, as expected for moieties with considerable flexibility. In compounds **1**, **9** and **10** the butyl tail was sometimes oriented into the bulk, thereby weakening its hydrophobic interaction with the UMA binding site. This indicates that the architecture of the compounds needs to enable favorable hydrophobic interaction of the tail with the enzyme if the inhibitors in this series are to induce significant biological activity. These structural features can be linked to the calculated partial binding free energies. Compounds **4**, **8** and **12** with cyclic substituents exhibited less flexibility during the MD runs, which leads to more beneficial hydrophobic interaction. Two of these inhibitors (**4** and **12**) also possess structural elements facilitating additional interaction with Thr36. In compound **4** the interactions of cyano nitrogen with the side chain oxygen and backbone nitrogen of Thr36 are favorable, with average distances of 3.04 and 3.36 Å, respectively, anchoring the compound firmly in the UMA binding site. The 2*H*-1,3-thiazine-2,6(3*H*)-dione group of compound **12** was initially positioned to form hydrogen bonds between the cyclic amide nitrogen and side chain oxygen of Thr36, and between the neighboring carbonyl oxygen and backbone nitrogen of Thr36. These interactions do not appear as favorable, since average distances of 5.30 and 6.23 Å were obtained.

Conclusions

Linear interaction energy (LIE) calculations of binding free energies were applied to a series of *N*-sulfonyl-glutamic acid inhibitors of MurD ligase. The optimized values of empirical coefficients of the LIE method $\alpha = 0.176$ and $\beta = 0.060$ were derived for this system. Decomposition of interaction energy into electrostatic and van der Waals contributions revealed non-polar interactions as the predominant driving force for the binding of these inhibitors, with electrostatics playing a minor role. However, the observed hydrogen bonding network provides evidence that electrostatic interactions enable proper orientation of the ligands in the active site [41].

The ability to exactly dissect the free energy into components arising from different groups of atoms or types of interactions within the LIE formalism enabled explicit evaluation of contributions of four structural moieties to the overall inhibitory activity. Binding free energies of three selected moieties – D-Glu, sulfonamide and naphthalene – were virtually identical in all investigated compounds. The binding contributions of the lipophilic tail allowed for discrimination between the inhibitors and additional correlation with the experimental values.

Analysis of MD trajectories corroborated well with the free energy calculations and enabled recognition of important structural features for inhibitory activity. The significance of favorable hydrophobic interactions between the lipophilic tail and the UMA binding site was revealed as a prerequisite for inhibitory activity when comparing five derivatives containing the butyl group. Applications of this type of complex all-atom model development pave the way and present a valid lead for somewhat less rigorous and considerably faster LIECE approach [40–42]. Quantitative evaluation of binding free energies in the *N*-sulfonylglutamic derivative series provides valuable clues to assist the lead optimization process of MurD inhibitors leading to novel antibacterial drugs.

References

1. Silver LL (2006) Does the cell wall of bacteria remain a viable source of targets for novel antibiotics? Biochem Pharmacol 71:996–1005
2. Brown ED, Wright GD (2005) New targets and screening approaches in antimicrobial drug discovery. Chem Rev 105:759–774
3. Vollmer W, Blanot D, de Pedro MA (2008) Peptidoglycan structure and architecture. FEMS Microbiol Rev 32:149–167
4. Barreteau H, Kovač A, Boniface A, Sova M, Gobec S, Blanot D (2008) Cytoplasmic steps of peptidoglycan biosynthesis. FEMS Microbiol Rev 32:168–207
5. van Heijenoort J (2001) Recent advances in the formation of the bacterial peptidoglycan monomer unit. Nat Prod Rep 18:503–519
6. Smith CS (2006) Structure, function and dynamics in the *mur* family of bacterial cell wall ligases. J Mol Biol 362:640–655
7. Bertrand JA, Auger G, Martin L, Fanchon E, Blanot D, Le Beller D, van Heijenoort J, Dideberg O (1999) Determination of the MurD mechanism through crystallographic analysis of enzyme complexes. J Mol Biol 289:579–590
8. Anderson MS, Eveland SS, Onishi H, Pompliano DL (1996) Kinetic mechanism of the Escherichia coli UDPMurNAc-tripeptide D-alanyl-D-alanine-adding enzyme: use of a glutathione S-transferase fusion. Biochemistry 35:16264–16269
9. Emanuele JJ Jr, Jin H, Yanchunas J , Villafranca JJ (1997) Evaluation of the kinetic mechanism of Escherichia coli uridine

diphosphate-N-acetylmuramate:L-alanine ligase. Biochemistry 36:7264–7271

10. Perdih A, Hodoscek M, Solmajer T (2009) MurD ligase from *E. coli*: Tetrahedral intermediate formation study by hybrid quantum mechanical/molecular mechanical replica path method. Proteins: Structure Funct Bioinf 74:744–759

11. Bouhss A, Dementin S, van Heijenoort J, Parquet C, Blanot D (2002) MurC and MurD synthetases of peptidoglycan biosynthesis: Borohydride trapping of acyl-phosphate intermediates. Methods in Enzymology 354:189–196

12. Falk PJ, Ervin KM, Volk KS, Ho H-T (1996) Biochemical evidence for the formation of a covalent acyl-phosphate linkage between UDP-*N*-Acetylmuramate and ATP in the *Escherichia coli* UDP-*N*-acetylmuramate:L-alanine ligase-catalyzed reaction. Biochemistry 35:1417–1422

13. Bertrand JA, Fanchon E, Martin L, Chantalat L, Auger G, Blanot D, van Heijenoort J, Dideberg O (2000) "Open" structures of MurD: domain movements and structural similarities with folylpolyglutamate synthetase. J Mol Biol 301:1257–1266

14. Perdih A, Kotnik M, Hodoscek M, Solmajer T (2007) Targeted Molecular Dynamics Simulation Studies of Binding and Conformational Changes in *E.Coli* MurD. Proteins: Structure Funct Bioinf 68:243–254

15. Zoeiby AE, Sanschagrin F, Levesque RC (2002) Structure and function of the Mur enzymes: Development of novel Inhibitors. Mol Microbiol 47:1–12

16. Tanner ME, Vaganay S, van Heijenoort J, Blanot D (1996) Phosphinate inhibitors of the D-glutamic acid-adding enzyme of peptidoglycan biosynthesis. J Org Chem 61:1756–1760

17. Štrancar K, Blanot D, Gobec S (2006) Design, synthesis and structure–activity relationships of new phosphinate inhibitors of MurD. Bioorg Med Chem 16:343–348

18. Humljan J, Kotnik M, Boniface A, Šolmajer T, Urleb U, Blanot D, Gobec S (2006) A new approach towards peptidosulfonamides: synthesis of potential inhibitors of bacterial peptidoglycan biosynthesis enzymes MurD and MurE. Tetrahedron 62:10980–10988

19. Humljan J (2007) Design, synthesis and characterization of new sulfonamide inhibitors of Mur ligases. PhD dissertation Ljubljana

20. Humljan J, Kotnik M, Contreras-Martel C, Blanot D, Urleb U, Desssen A, Solmajer T, Gobec S (2008) Novel naphtalene – N-sulfonyl-D-glutamic acid derivatives as inhibitors of MurD, a key peptidoglycan biosynthesis enzyme. J Med Chem 51:7486–7494

21. Pratviel-Sosa F, Acher F, Trigalo F, Blanot D, Azerad R, van Heijenoort J (1994) Effect of various analogues of D-glutamic acid on the D-glutamate-adding enzyme from Escherichia coli. FEMS Microbiol Lett 115:223–228

22. Kotnik M (2007) Computer-Aided and Structure-Based Design of Novel Inhibitors of Mur Ligases. PhD dissertation Ljubljana

23. Kotnik M, Humljan J, Contreras-Martel C, Oblak M, Kristan K, Hervé M, Blanot D, Urleb U, Gobec S, Dessen A, Solmajer T (2007) Structural and functional characterization of enantiomeric glutamic acid derivatives as potential transition state analogue inhibitors of MurD ligase. J Mol Biol 370:107–115

24. Obreza A, Gobec S (2004) Recent advances in design, synthesis and biological activity of aminoalkylsulfonates and sulfonamidopeptides. Curr Med Chem 11:3263–3278

25. Jorgensen WL (2004) The Many Roles of Computation in Drug Discovery. Science 303:1813–1818

26. Klebe G (2006) Virtual ligand screening: strategies, perspectives and limitations. Drug Discovery Today 11:580–594

27. Schneider G, Böhm H-J (2002) Virtual screening and fast automated docking methods. Drug Discovery Today 7:64–70

28. Wolber G, Langer T (2005) LigandScout: 3-D pharmacophores derived from protein-bound ligands and their use as virtual screening filters. J Chem Inf Model 45:160–169

29. Kollman PA (1993) Free energy calculations: Applications to chemical and biochemical phenomena. Chem Rev 93:2395–2417

30. Chen X, Tropsha A (2006) Calculation of the relative binding affinity of enzyme inhibitors using the generalized linear response method. J Chem Theory and Comput 2:1435–1443

31. Åqvist J, Medina C, Samuelson JE (1994) A new method for predicting binding affinity in computer-aided drug design. Protein Eng 7:385–391

32. Åqvist J, Luzhkov VB, Brandsdal BO (2002) Ligand Binding Affinities from MD Simulations. Acc Chem Res 35:358–365

33. Florián J, Goodman MF, Warshel A (2002) Theoretical investigation of the binding free energies and key substrate-recognition components of the replication fidelity of human DNA polymerase β. J Phys Chem B 106:5739–5753

34. Lee FS, Chu Z-T, Bolger MB, Warshel A (1992) Calculations of antibody-antigen interactions: microscopic and semi-microscopic evaluation of the free energies of binding of phosphorylcholine analogs to McPC603. Protein Eng 5:215–228

35. Bren U, Martinek V, Florian J (2006) Free energy simulations of uncatalyzed DNA replication fidelity: Structure and stability of T·G and dTTP·G terminal DNA mismatches flanked by a single dangling nucleotide. J Phys Chem B 110:10557–10566

36. Carlson HA, Jorgensen WL (1995) An extended linear response method for determining free energies of hydration. J Phys Chem 99:10667–10673

37. Zhou RH, Friesner RA, Ghosh A, Rizzo RC, Jorgensen WL, Levy RM (2001) New Linear interaction method for binding affinity calculations using a continuum solvent model. J Phys Chem B 105:10388–10397

38. Smith RH, Jorgensen WL, Tirado-Rives J, Lamb ML, Janssen PAJ, Michejda CJ, Smith MBK (1998) Prediction of binding affinities for TIBO inhibitors of HIV-1 reverse transcriptase using Monte Carlo simulations in a linear response method. J Med Chem 41:5272–5286

39. Hansson T, Marelius J, Aquist J (1998) Ligand binding affinity prediction by linear interaction energy methods. J Comp–Aid Mol Des 12:27–35

40. Carlson J, Boukharta L, Aquist J (2008) Combining Docking, Molecular Dynamics and the Linear Interaction Energy Method to Predict Binding Modes and Affinities for Non-nucleoside Inhibitors to HIV-1 Reverse Transcriptase. J Med Chem 51:2648–2656

41. Kolb P, Huang D, Dey F, Caflisch A (2008) Discovery of kinase inhibitors by high-throughput docking and scoring based on a transferable linear interaction energy model. J Med Chem 51:1179–1188

42. Bortolato A, Moro S (2007) In silico binding free energy predictability by using the linear interaction energy (LIE) method: Bromobenzimidazole CK2 inhibitors as a case study. J Chem Inf Model 47:572–582

43. Foloppe N, Hubbard R (2006) Towards predictive ligand design with free-energy based computational methods? Curr Med Chem 13:3583–3608

44. Bren M, Florián J, Mavri J, Bren U (2007) Do all pieces make a whole? Thiele cumulants and the free energy decomposition. Theor Chem Acc 117:535–540

45. http://www.pdb.org/pdb/.

46. Borštnik U, Hodošček M, Janežič D (2004) Improving the performance of molecular dynamics simulations on parallel clusters. J Chem Inf Comput Sci 44:359–364

47. Marelius J, Kolmodin K, Feierberg I, Åqvist J (1999) A molecular dynamics program for free energy calculations and empirical

valence bond simulations in biomolecular systems. J Mol Graphics Model 16:213–225

48. Cornell WD, Cieplak P, Bayly CI, Gould IR, Merz M Jr, Ferguson DM, Spellmeyer DC, Fox T, Caldwell JW, Kollman PA (1995) A second generation force field for the simulation of proteins, nucleic acids, and organic molecules. J Am Chem Soc 117:5179–5197

49. Spartan 5.0 Wavefunction In Irvine CA USA

50. Gaussian 03 Revision C.02 Frisch M J, Trucks GW, Schlegel HB, Scuseria GE, Robb MA, Cheeseman JR, Montgomery J A, Vreven T Jr, Kudin KN, Burant JC, Millam JM, Iyengar SS, Tomasi J, Barone V, Mennucci B, Cossi M, Scalmani G, Rega N, Petersson GA, Nakatsuji H, Hada M, Ehara M, Toyota K, Fukuda R, Hasegawa J, Ishida M, Nakajima T, Honda Y, Kitao O, Nakai H, Klene M, Li X, Knox JE, Hratchian HP, Cross JB, Bakken V, Adamo C, Jaramillo J, Gomperts R, Stratmann RE, Yazyev O, Austin AJ, Cammi R, Pomelli C, Ochterski JW, Ayala PY, Morokuma K, Voth GA, Salvador P, Dannenberg JJ, Zakrzewski VG, Dapprich S, Daniels AD, Strain MC, Farkas O, Malick DK, Rabuck AD, Raghavachari K, Foresman JB, Ortiz JV, Cui Q, Baboul AG, Clifford S, Cioslowski J, Stefanov BB, Liu G, Liashenko A, Piskorz P, Komaromi I, Martin RL, Fox DJ, Keith T, Al-Laham MA, Peng CY, Nanayakkara A, Challacombe M, Gill PMW, Johnson B, Chen W, Wong MW, Gonzalez C, Pople JA Gaussian Inc., Wallingford, CT 2004

51. Bren U, Hodoscek M, Koller J (2005) Development and Validation of Empirical Force Field Parameters for Netropsin. J Chem Inf Model 45:1546–1552

52. Bayly CI, Cieplak P, Cornell WD, Kollman PA (1993) A well-behaved electrostatic potential based method using charge restrains for deriving atomic charges: The RESP Model. J Phys Chem 97:10269–10280

53. Jorgensen WL, Chandrasekhar J, Madura JD, Impey RW, Klein ML (1983) Comparison of simple potential functions for simulating liquid water. J Chem Phys 79:926–935

54. King G, Warshel A (1989) A surface constrained all-atom solvent model for effective simulations of polar solutions. J Chem Phys 91:3647–3661

55. Lee FS, Warshel A (1992) A local reaction field method for fast evaluation of long-range electrostatic interactions in molecular simulations. J Chem Phys 97:3100–3107

56. Handler N, Brunhofer G, Studenik C, Leisser K, Jaeger W, Parth S, Erker T (2007) 'Bridged' stilbene derivatives as selective cyclooxygenase-1 inhibitors. Bioorg Med Chem 15:6109–6118

57. Humphrey W, Dalke A, Schulten K (1996) VMD: visual molecular dynamics. J Mol Graph 14:33–38

58. Gramatica P (2007) Principles of QSAR models validation: internal and external. QSAR Comb Sci 26:694–701